

where  $R = Q(1 - Q)^{-2}$

$$(\partial P / \partial y)_{T,V} = T(\gamma V)^{-1}[\frac{2}{3}R - (2\gamma/T)(3A\Phi - B)\Phi] \quad (A4)$$

$$(\partial y / \partial V)_T = \{(\gamma/V)[\frac{2}{3}R - (2\gamma/T)(3A\Phi - B)\Phi] / \{\frac{4}{3}R + (\gamma/2T)(9A\Phi - 2B)\Phi + (s/c)[y^{-1} \ln(1 - y) + (1 - y)^{-1}]\}\} \quad (A5)$$

Differentiation of (A3), (A4), and (A5) gives

$$(\partial^2 P / \partial V^2)_{T,y} = (T/V^3)[PV/T + (R/9)(7 - 5Q) \times (1 - Q)^{-1} + (2\gamma/T)(24A\Phi - 8B)\Phi - (V^2/T)(\partial P / \partial V)_{T,y}] \quad (A6)$$

$$(\partial^2 P / \partial V \partial y)_T = [T/(\gamma V^2)][(2\gamma/T)(12A\Phi - 2B)\Phi - \frac{2}{9}R(1 + Q)(1 - Q)^{-1} - (\gamma V/T)(\partial P / \partial y)_{V,T}] \quad (A7)$$

$$(\partial^2 P / \partial y^2)_{T,V} = [T/(\gamma^2 V)][(4\gamma/T)(6A\Phi - B)\Phi - \frac{2}{9}R(1 - 5Q)(1 - Q)^{-1}] \quad (A8)$$

$$(\partial^2 y / \partial V^2)_T \{\frac{4}{3}R + (\gamma/2T)(9A\Phi - 2B)\Phi + (s/c)[y^{-1} \ln(1 - y) + (1 - y)^{-1}]\} = (\gamma/V^2)[(\gamma/2T)(60A\Phi - 12B)\Phi - \frac{4}{9}R(2 - Q)(1 - Q)^{-1} + (1/V)(\partial y / \partial V)_T[(\gamma/2T)(60A\Phi - 4B)\Phi + \frac{2}{9}R(7 + Q)(1 - Q)^{-1}] + (1/\gamma)[(\partial y / \partial V)_T]^2[(\gamma/2T)(27A\Phi - 2B)\Phi - \frac{8}{9}R(1 + Q)(1 - Q)^{-1} + (s/c)[y^{-1} \ln(1 - y) + (1 - 2\gamma)(1 - y)^{-2}]] \quad (A9)$$

Insertion of the appropriate quantities in (A1) and (A2) and some further simplification yield eq 9, 11, and 12.

## References and Notes

- (1) Prigogine, I.; Trappeniers, N.; Mathot, V. *Discuss. Faraday Soc.* **1953**, *15*, 93.
- (2) Flory, P. J.; Orwoll, R. A.; Vrij, A. *J. Am. Chem. Soc.* **1964**, *86*, 3507.
- (3) Sanchez, I. C.; Lacombe, R. H. *J. Phys. Chem.* **1976**, *80*, 2352.
- (4) Kleintjens, L. A.; Koningsveld, R. *Colloid Polym. Sci.* **1980**, *258*, 711.
- (5) Simha, R.; Somcynsky, T. *Macromolecules* **1969**, *2*, 342.
- (6) Zoller, P. *J. Polym. Sci., Polym. Phys. Ed.* **1980**, *18*, 157, 897.
- (7) Dee, G. T.; Walsh, D. J. *Macromolecules* **1988**, *21*, 811.
- (8) Nies, E.; Kleintjens, L. A.; Koningsveld, R.; Simha, R.; Jain, R. K. *Fluid Phase Equilib.* **1983**, *12*, 11.
- (9) Nies, E.; Van der Haegen, R. *Macromolecules* **1988**, *21*, 2633.
- (10) For example: Jain, R. K.; Simha, R. *Macromolecules* **1980**, *13*, 1501, with references to previous papers.
- (11) Arbuzova, A. P.; Besklubenko, Yu. D.; Lipatov, Yu. S.; Privalko, V. P.; Pasko, S. P.; Fedorova, N. *Polym. Sci. USSR* **1983**, *25*, 1055.
- (12) Zoller, P.; Jain, R. K.; Simha, R. *J. Polym. Sci., Polym. Phys. Ed.* **1986**, *24*, 687.
- (13) Simha, R. *Macromolecules* **1977**, *10*, 1025.
- (14) Simha, R.; Wilson, P. S. *Macromolecules* **1973**, *6*, 908.
- (15) McKinney, J. E.; Simha, R. *Macromolecules* **1974**, *7*, 894.
- (16) Jain, R. K. *Fluid Phase Equilib.* **1984**, *15*, 323.
- (17) Hartmann, B.; Simha, R.; Berger, A. E. *J. Appl. Polym.*, in press.
- (18) Cutler, W. G.; McMickle, R. H.; Webb, W.; Schiessler, R. W. *J. Chem. Phys.* **1958**, *29*, 727.
- (19) Simha, R.; Hadden, S. T. *J. Chem. Phys.* **1956**, *25*, 702.
- (20) Nanda, V. S.; Simha, R. *J. Chem. Phys.* **1964**, *41*, 1884.
- (21) Olabisi, O.; Simha, R. *J. Appl. Polym. Sci.* **1977**, *21*, 149.
- (22) Quach, A.; Simha, R. *J. Appl. Phys.* **1971**, *42*, 4592.
- (23) Jain, R. K.; Simha, R. *J. Chem. Phys.* **1979**, *70*, 2792.

## A Study of Single-Arm Relaxation in a Polystyrene Star Polymer by Neutron Spin Echo Spectroscopy

D. Richter\* and B. Farago

Institut Laue-Langevin, 156X, 38042 Grenoble Cedex, France

J. S. Huang and L. J. Fetters

Exxon Research and Engineering Co., Rt. 22E, Annandale, New Jersey 08801

B. Ewen

Max Planck Institut für Polymerforschung, 6500 Mainz, FRG. Received February 3, 1988; Revised Manuscript Received June 21, 1988

**ABSTRACT:** We have studied 12-arm polystyrene star molecules by elastic and quasi-elastic small-angle neutron scattering. Labeling single arms, we accessed the static and dynamic properties of the star constituents and compared the results with those from a fully labeled star. While the collective dynamic response is characterized by a strong minimum in the reduced relaxation rate, this minimum is absent in the single-arm response. Consequently, the minimum originates from interarm interactions in accordance with its previous characterization as a de Gennes type narrowing.

A star polymer is a macromolecule consisting of many ( $\geq 3$ ) linear homopolymers of nearly identical molecular weight, chemically linked to a common seed molecule which extends no more than a few bond lengths. The presence of the star center implies a strong stretching of the chains due to the crowding of arms near the center region and the subsequent relaxation toward the rims. Thus a star polymer may in a single structure contain monomer concentrations ranging all the way from that of the melt to that of a dilute solution. Even though the

behavior of the linear polymers has been successfully described by the scaling theories in general terms, much less is known concerning the properties of a star polymer of finite size. Recently, it has been possible to synthesize monodispersed model star polymers by anionic polymerization. There has been an intense effort in the study of this new class of well-characterized polymers. These efforts include the long-standing theoretical investigations,<sup>1,2</sup> as well as experimental studies by static and dynamic light scattering,<sup>3</sup> small-angle neutron scattering,<sup>4,5</sup> quasi-elastic

neutron scattering,<sup>5</sup> dilute solution viscosity,<sup>6</sup> and computer simulations.<sup>7</sup>

In particular, neutron scattering techniques have proved to be especially suitable for the study of hydrocarbon systems which include most of the polymers and polymer solutions. This is partly due to the fact that the wavelength of the cold neutrons is just of the order of a monomer size and more specifically due to the large difference in the coherent scattering length of the hydrogen atom and its isotope deuterium. By judicious substitution of the hydrogen by deuterium, either in the polymer molecules or in the solvents, one can obtain a large contrast for the scattering process of specific interest.

Richter et al. have recently studied the dynamics of dilute polyisoprene star polymers in perdeuterated benzene employing the neutron spin-echo technique.<sup>5</sup> In these measurements the polymer relaxation function is measured as a function of the momentum transfer  $Q$  during scattering ( $Q = 4\pi/\lambda \sin \theta$ , where  $\lambda$  is the neutron wavelength and  $2\theta$  the scattering angle). They found that compared to that of a linear chain the internal relaxation rate  $\Omega$  is strongly reduced, if the value of  $QR_g$  is in the neighbourhood of  $1.5-R_g$ , thereby, denotes the radius of gyration of the star polymer arms. Since for Zimm relaxation of linear polymers  $\Omega$  scales with  $Q^3$ , it is convenient to consider reduced relaxation rates  $\Omega/Q^3$ , thus taking out the ordinary Zimm behavior. This reduced rate was found to scale with the variable  $QR_g$ , independent of the molecular weight of the polymer star. At  $QR_g \gg 1$ , from scaling arguments one finds that  $\Omega \sim Q^3$ , independent of the molecular weight or the branching. It is found that the reduced rates  $\Omega/Q^3$  for both the star-branched polyisoprenes (of various degrees of branching) and the linear polyisoprene tend to the same limit at large  $Q$  determined only by the friction term:  $T/\eta$  ( $T$  is the absolute temperature and  $\eta$  is the viscosity of the solvent). For  $QR_g < 1$ , one expects all the internal dynamics to disappear from the quasi-elastic neutron scattering, leaving only the diffusive modes of the center of mass of the polymer molecules. Since in this limit,  $\Omega \sim kTQ^2(2^{1/2} + f)/R_g f$ ,<sup>8</sup>  $\Omega/Q^3$  scales again with  $QR_g$ . Apart from numerical factors the proportionality constant is given by  $T/\eta$  and depends weakly on  $f$ . Thus all line-width measurements at a given functionality are expected to converge into a universal curve at low values of  $Q$ . With increasing functionality also the  $f$ -dependence drops out quickly. In the crossover regime from translational diffusion ( $\Omega \sim Q^2$ ) to Zimm dynamics ( $\Omega \sim Q^3$ ), however, the star branched polymer behavior differs strongly from the behavior of the linear polymer. The measured reduced line width  $\Omega/Q^3$  for the star polymers exhibits a pronounced minimum before it reaches the high- $Q$  plateau value. The position of the minimum is observed near  $QR_g \simeq 1.5$ . This slowing down of the dynamics occurs in the neighborhood of the maximum in the Kratky plot of the scaled intensity (where  $IQ^2$  is plotted as a function of  $QR_g$ ). This maximum in the Kratky plot is characteristic for branched polymers but absent from the scattering of linear polymers. It arises as a consequence of an enhanced radial monomer distribution function at a distance  $r \simeq R_g$ . This is the reason why the minimum in the measured line width of the star polymers has been associated with a "de Gennes narrowing"-like process observed in liquids.<sup>9</sup> There, the so-called de Gennes narrowing approximates the effect of pairwise interactions by a normalization of the relaxation rates with the static structure factor  $S(Q)$ —correlations which are preferred by a system live longer. It should be noted, however, that, unlike to the case of a de Gennes narrowing,

**Table I**  
Polystyrene Star Molecules Used in the Experiments; the  $R_g$  Values Were Obtained from Neutron Small-Angle Scattering

sample	$10^{-4}M_w$	$R_g$ , Å	solvent	method
PS 4-12	46.7	127	toluene <sup>12</sup>	Guinier regime
PS 6-12	14.9	73	toluene <sup>12,13</sup>	Guinier regime
		70	THF	peak in Kratky plot
PS120A	14.9	63	THF- <i>d</i>	Guinier regime

for the star polymer solution at the concentration of interest (below the overlap concentration  $c^*$ ), neither the scattering structure factor arising from mutual interaction between different stars nor the single-star scattering form factor show any discernible peak at  $QR_g \simeq 1$ . Thus, the minimum in the  $\Omega/Q^3$  versus  $Q$  plot for the dilute star solution does not arise from the interparticle interaction but rather from the interactions between the arms in the same star structure. The mechanism of this rate reduction is either related to the influence of the center of the star on fluctuations of the range of  $R_g$ , or it is due to enhanced correlation of monomer densities in the single star over distances roughly equal to  $R_g$ .

In order to gain further insight into the physics behind the minimum in the scaled line width, we have performed static and dynamic measurements on a single labeled arm within a 12-arm polystyrene star molecule in dilute solution. For comparison we studied an identical fully labeled star. Furthermore the molecular weight scaling behavior was reinvestigated, studying fully labeled 12-arm stars of different sizes.

The chemical synthesis of 12-arm PS star molecules has been described in the literature.<sup>6,10</sup> It bases an organolithium anionic polymerization using tetrakis(trichlorosilyl)ethylsilane as a linking agent. The PS stars with a single labeled arm were prepared starting the linking reaction in a 11:1 mixture of deuterated and protonated precursor PS chains. From this procedure it is clear that only on the average one-arm labeled stars were created, while in reality the number of labeled arms in a star is distributed according to a binomial distribution. Accordingly more than 92% of all the stars have either 0 or 1 or 2 arms. All star polystyrenes were fractionated (using toluene/methanol as the solvent/nonsolvent) in order to eliminate the remaining linear polymers. Characterization of the star arms and the fractional stars was done by a combination of size-exclusion chromatography, low-angle laser light scattering, and osmometry. The fractionated samples showed  $M_z/M_w$  and  $M_w/M_n$  ratios of  $<1.1$ . The polymers used in our experiments are listed in Table I.

The comparison between the one arm and the fully labeled star was performed on the two differently labeled 12-arm PS stars of identical molecular weight (PS120A and PS6-12). They were dissolved in deuterated THF ( $C_4D_8O$ ) the scattering length density of which nearly exactly matches that of deuterated PS. The neutron small-angle scattering (SANS) experiments were carried out by using the small-angle scattering apparatus D17 at the Institut Laue-Langevin (ILL) in Grenoble. The PS120A star was investigated at three different monomer concentrations ( $c = 1\%$ ,  $2\%$ , and  $3\%$ ), while the fully protonated PS6-12 star was investigated only at  $c = 1\%$ . The data were corrected for background and calibrated to a measurement on a 1-mm water cell. For the single-arm labeled sample no concentration dependence was observed. Figure 1 presents the data from the fully protonated star in a Kratky representation. ( $IQ^2$  vs  $Q$ ). As a signature of the star architecture, the data show a pronounced peak occurring at  $Q = 2.9 \cdot 10^{-2} \text{ Å}^{-1}$ .

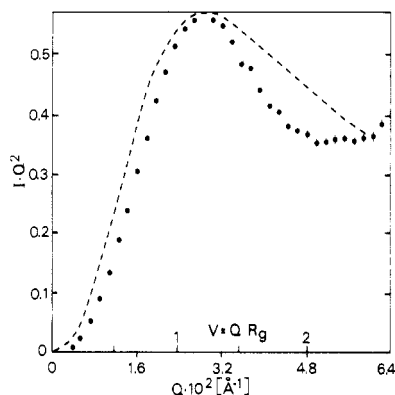


**Figure 1.** SANS data from the fully protonated 12-arm polystyrene star PS6-12 ( $M_w = 1.49 \times 10^5$ ) in dilute solution of THF ( $c = 1\%$ ). The data are shown in a Kratky representation ( $IQ^2$  vs  $Q$ ). The dashed line displays the prediction of eq 1 adapted to the maximum.

For a star built from Gaussian chains Benoit has derived the static form factor  $P(Q)^{11}$

$$P(Q) = \frac{2N}{fv^4} \left\{ v^2 - [1 - \exp(-v^2)] + \frac{f-1}{2} [1 - \exp(-v^2)]^2 \right\} \quad (1)$$

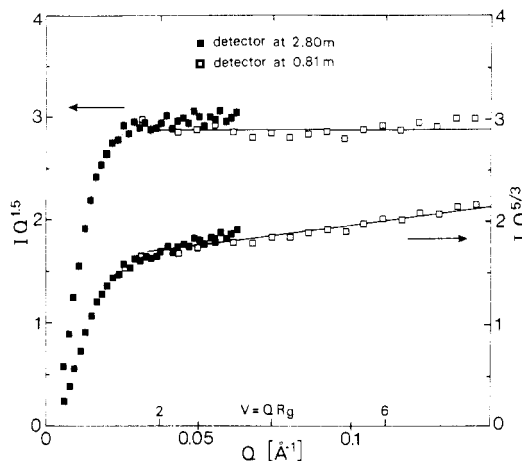
Here  $f$  is the functionality of the star and  $v = QR_g$ . The radius of gyration of the whole star  $\tilde{R}_g$  is related to that of one arm by

$$\tilde{R}_g^2 = (3f - 2)/f R_g^2 \quad (2)$$

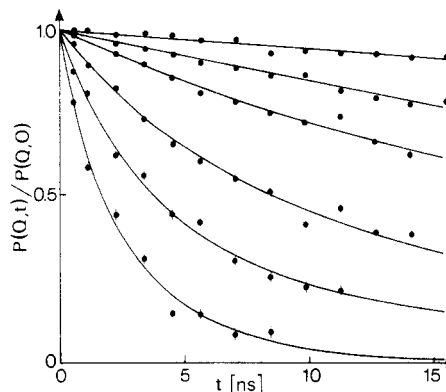
For  $f = 12$ ,  $P(Q)$  exhibits a maximum around  $v = 1.2$ . Using the experimental  $Q_{\max} = 2.9 \times 10^{-2} \text{ Å}^{-1}$  we find  $\tilde{R}_g = 70 \text{ Å}$ , in very good agreement with a value of  $73 \text{ Å}$  obtained from the Guinier regime in toluene.<sup>10</sup> We note that our data did not allow the extraction of  $\tilde{R}_g$  from the Guinier range. Most likely the concentration of 1% caused already some interstar interferences at the smallest  $Q$ . While the predicted position of the maximum in the Kratky plot agrees well with measured radius of gyration, the experimentally observed line shape disagrees strongly with the prediction of eq 1 as shown by a dashed line in Figure 1. While the width of the peak according to eq 1 amounts to  $\Delta v \approx 1.5$ , experimentally we observe about half this value. This is in contrast to early observations<sup>5</sup> on high-functionality polyisoprene stars where an agreement with eq 1 also with respect to the line shape was found.

Figure 2 displays the SANS data from the one-arm labeled stars (PS120A). In order to demonstrate the asymptotic (large  $Q$ ) behavior, we have plotted both  $IQ^{1.5}$  and  $IQ^{5/3}$  vs  $Q$ . While the plot of  $IQ^{1.5}$  vs  $Q$  achieves a high  $Q$  plateau, such a plateau is not reached for the scaling appropriate for a swollen coil. The observed considerable deviation toward a lower exponent indicates strongly stretched arms. This observation finds its counterpart in recent molecular dynamics simulations on star molecules which also found stretched configurations with a  $Q$  scaling on the order of  $Q^{-1.5}$ .<sup>7</sup> Finally concerning the radius of gyration of the labeled arm, in the Guinier regime we obtain  $R_g \approx 63 \text{ Å}$ . Applying eq 2 which relates  $\tilde{R}_g$  and  $R_g$  and inserting the measured value for the full star of  $\tilde{R}_g = 70 \text{ Å}$ ,<sup>10</sup> we obtain the much smaller value of  $R_g = 43 \text{ Å}$ . This large discrepancy may partly result from the stretched chain conformations. However, since our sample contains an important admixture of stars with two labeled arms, an experimentally clear statement on  $R_g$  for one arm cannot be made.

The quasi-elastic neutron scattering experiments were performed on the spin-echo spectrometer IN11 at the ILL.



**Figure 2.** SANS data from the 12-arm polystyrene star PS120A ( $M_w = 1.49 \times 10^5$ ) where the 11 deuterated arms were matched by the solvent THF. In order to demonstrate the asymptotic  $Q$  behavior, the data are plotted in a generalized Kratky representation ( $IQ^\alpha$  vs  $Q$  with  $\alpha = 1.5$  and  $5/3$ ). The solid line marks the high- $Q$  plateau.



**Figure 3.** Neutron spin-echo spectra obtained from the one-arm labeled PS star PS120A in deuterated THF. The solid lines are a result of a fit with the dynamic structure factor  $P_{DG}(Q,t)$  calculated by Dubois-Violette and de Gennes.<sup>15</sup> The above data represent the following values of  $Q$ : 0.026, 0.040, 0.053, 0.079, 0.106, 0.132  $\text{Å}^{-1}$ .

The incident neutron wavelength was  $\lambda = 8.3 \text{ Å}$  with a fwhm of approximately 16.5%. In a quasi-elastic neutron scattering experiment the dynamics of the scattering system are obtained from the probability of detecting a scattered neutron with a given energy change. (For neutrons, the energy change is related to a velocity change.) The neutron spin-echo measurements determine directly the change of velocity of each individual neutron involved in the scattering process. This is achieved by measuring the difference of the phase angle of the neutron spin processing in a homogenous guide field  $H$  before and after the individual scattering events. The measured final neutron polarization  $P(Q,H)$ , thereby, is apart from resolution effects directly given by the real part of the normalized intermediate scattering function  $P(Q,t)/P(Q,0)$ , the time being proportional to  $H$ .<sup>14</sup>

In Figure 3 we present selected neutron spin-echo spectra obtained from the one-arm labeled PS star (PS120A) in 5% solution in deuterated THF. The data were corrected for solvent scattering and resolution. The solid lines fitted to the measured points are calculated by using an expression for the dynamic form factor  $P_{DG}(Q,t)$  derived by Dubois-Violette and de Gennes for linear polymers in dilute solution.<sup>15</sup> The line shape observed for the star polymer apparently agrees well with the theory. From the fit with  $P_{DG}(Q,t)$  we obtain a relaxation rate  $\Omega$

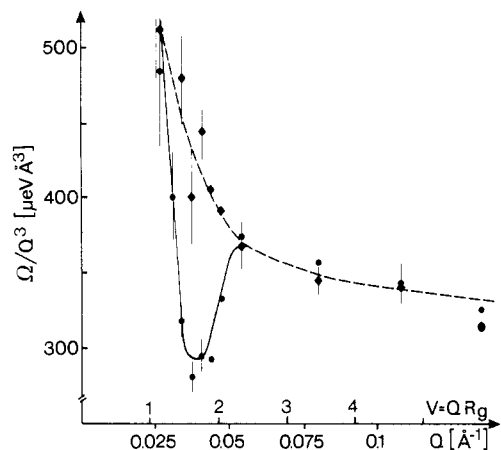


**Figure 4.** Reduced relaxation rates  $\Omega/Q^3$  for the fully protonated (●) and the one-arm labeled star (◆) as a function of  $Q$ . The lines are guides to the eye.

for each scattering angle. In Figure 4 we show a comparison between the reduced rate  $\Omega/Q^3$  obtained for the whole star (closed circles) and that for the single protonated arm in an otherwise deuterated star in the matching deuterated solvent. We emphasize the following features in Figure 4: First, there exists a minimum of the reduced rate in the 12-arm star, but the minimum is absent for the one-arm labeled sample. Otherwise, the limiting behavior  $\Omega/Q^3$  for the two systems is the same. Second, the minimum appears to be much narrower ( $\Delta QR_g \approx 0.6$ ) than that observed in the polyisoprene systems ( $\Delta QR_g \approx 1.5$ ). Third, the crossover of  $\Omega$  from the  $Q^2$  to  $Q^3$  dependence for the labeled arm in the star architecture is apparently much more gentle than that observed for an unattached linear polystyrene chain. We shall devote the remainder of this paper to a discussion of these features.

### The Minimum in the Reduced Rate

It is clear from the results obtained from star polymers containing one labeled arm that the  $\Omega/Q^3$  curve exhibits no minimum. We thus conclude that the slowing down of the star dynamics in the crossover regime is due to the collective motions of the arms at the length scale of  $R_g$ . This should be viewed as a consequence of the star structure, namely, that an enhanced monomer-monomer correlation exists at a distance of separation  $\sim R_g$ . This enhancement in turn causes a peak in the Kratky plot of the static form factor  $Q^2P(Q)$  at  $Q \approx 1/R_g$  and an increase of the osmotic compressibility of the monomers corresponding to a wavevector  $Q \sim 1/R_g$ .<sup>16</sup> This enhancement is mainly due to interarm correlations. Consequently, it affects primarily the collective dynamic response. In fact, as we have remarked earlier, the single-arm dynamics in the crossover regime shows just the opposite effect; i.e., the relaxation of the labeled arm is faster than that of a comparable free linear chain in the range  $Q \sim 1/R_g$ .

### The Narrowness of the Minimum

The minimum of the reduced rate observed for the polystyrene star appears to be significantly narrower than that of the polyisoprene system. Furthermore, the scaling behavior with respect to the radius of gyration is absent for the polystyrene stars. Figure 5 displays the reduced rate  $\Omega/Q^3$  for the 12-arm polystyrene stars of different molecular weight (PS6-12 and PS4-12) as a function of the scaling variable  $v$ . The larger molecular weight star was studied in toluene at 100 °C. In order to make the results for the two stars comparable, the magnitudes of  $\Omega/Q^3$  at large  $Q$  were adjusted to each other (multiplication of the PS6-12 results by 2.8). It is obvious that the decrease in

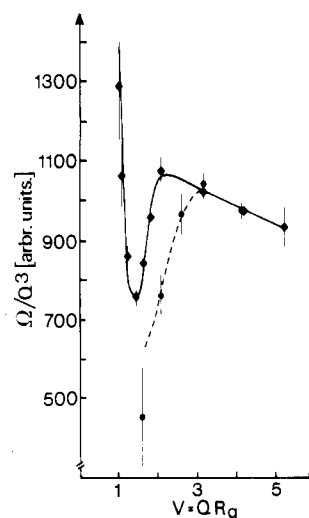


**Figure 5.** Reduced relaxation rates  $\Omega/Q^3$  for two PS stars at different molecular weights ((◆)  $M_w = 1.44 \times 10^5$ ; (●)  $M_w = 5.09 \times 10^5$ ) as a function of the scaling variable  $v$ . The lines are guides to the eye.

$\Omega/Q^3$  commences at larger values of  $v$  for the high  $M_w$  star. Because of the higher molecular weight (and thus large  $R_g$ ), the NSE spectrometer was not able to access a low enough  $Q$  range to see the full minimum of the reduced rate for the larger star. We relate this deviation from scaling to the existence of an additional length in the dynamics of polystyrene, which is important in the spatial range accessed by neutron spin-echo. As has been pointed out in the literature,<sup>7,8</sup> polystyrene has a rather low flexibility. Consequently, the influence of intramolecular steric hindrances or the intramolecular potential extends to rather long distances, thus introducing another length scale in the spatial range covered by NSE. On the other hand, for the flexible PIP<sup>9</sup> within the NSE range, universal behavior is already reached. We also remark that the peak in the Kratky plot for the PS star (Figure 1) is distinctly sharper than that for the PIP star.<sup>5</sup> In fact, if we measure the width of the Kratky peak halfway between the peak and the high- $Q$  plateau value in units of  $(\Delta QR_g)$ , we find that this width of the maximum for the polystyrene system is roughly one-half of that of the polyisoprene system. It is thus interesting to note that the width of the minimum of the scaled line width for the polystyrene stars is also just about one-half of that of the polyisoprene stars. Again this strongly suggests the connection between the Kratky peak and the slowing down of the relaxation rate, as one would expect from a de Gennes narrowing process.

### The Wide Crossover Regime Observed for the Labeled Arm

The crossover of  $\Omega$  from a  $Q^2$  to a  $Q^3$  dependence for linear polystyrene has been studied by Nicholson et al.<sup>20</sup> It was observed that this crossover regime was very narrow, as it was the case for the four-arm polyisoprene star measured by Richter et al.<sup>5</sup> However, if we replot the data for the one-arm labeled star of Figure 4 in terms of  $\Omega/Q^2$  vs  $Q$  (Figure 6), we realize that the crossover regime is very broad. At first sight, it is surprising that  $\Omega/Q^3$  increases above the high- $Q$  value before translational diffusion is reached. Intuitively one could have reasoned that beyond approximately  $R_g$  also the internal relaxation of a single arm should be retarded compared to that of a linear polymer, since beyond  $R_g$  the mean-square displacement of a given segment has to pull behind the whole star. However, on the other hand, as was seen in the SANS data (Figure 2), the single arm is considerably stretched com-

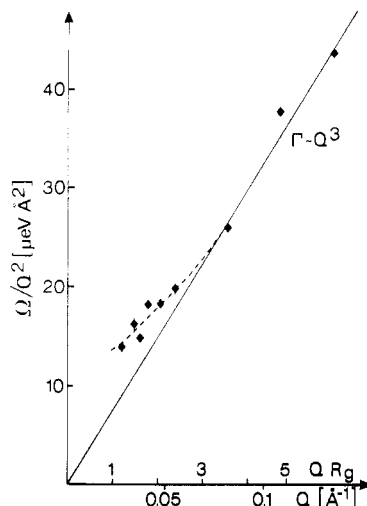


**Figure 6.** Reduced relaxation rates  $\Omega/Q^2$  obtained from the one-arm labeled star (PS120A) as a function of  $Q$  and  $\nu$ . The solid line represents the asymptotic  $Q^3$  behavior due to internal Zimm modes. The dashed line indicates the slow crossover to translational diffusion.

pared to a linear polymer ( $I \sim Q^{-1.5}$  instead of  $I \sim Q^{-5/3}$ ). Perhaps this gives rise to effectively stiffer segments as  $1/Q$  increases beyond a few bond lengths. The larger  $1/Q$ , the stiffer the mean segment, and the higher the characteristic frequency until  $1/Q \gg R_g$ . Then the center of mass diffusion dominates again.

In spite of the simple geometry of the multiarmed star branched polymer, the dynamics and structure of a finite size star polymer appear to be interesting and rich in physics. Through the advances in the modern synthetic chemistry, monodispersed star polymers with specific labeling by deuterium substitution can be produced. This allows the neutron scattering technique to probe not only the relation between structure and dynamics of the whole molecule but also any of the designated parts. We have learned that the characteristic minimum in the scaled line width of the collective relaxation of star polymers does not appear in the dynamics of a single-labeled arm in the star

structure. Furthermore, the polystyrene star does not seem to obey the scaling behavior observed in the polyisoprene systems. Nevertheless, the static form factors of the polystyrene star and its labeled arms reflect the anomaly of the observed dynamics. A more fundamental theoretical approach to these observations should prove useful for the understanding of not only the star polymers but also other branched system, including polymer networks.

**Registry No.** Neutron, 12586-31-1; polystyrene, 9003-53-6.

## References and Notes

- (1) For an overview, see, e.g.: Burchard, W. In *Advances in Polymer Science*; Cantow, H. J., et al., Eds.; Springer Verlag: Berlin, Heidelberg, New York, 1983; Vol. 48.
- (2) Daoud, M.; Cotton, J. P. *J. Phys. (Les Ulis, Fr.)* **1982**, *43*, 531.
- (3) Huber, K.; Burchard, W.; Fetters, L. J. *Macromolecules* **1984**, *17*, 541.
- (4) Dozier, W. D.; Huang, J. S.; Fetters, L. J., unpublished results.
- (5) Richter, D.; Stühn, B.; Ewen, B.; Nerger, D. *Phys. Rev. Lett.* **1987**, *58*, 2462.
- (6) Khasat, N.; Pennisi, R. W.; Hadjichristidis, N.; Fetters, L. J. *Macromolecules*, in press.
- (7) Grest, G. S.; Kremer, K.; Witten, T. A. *Macromolecules* **1987**, *20*, 1376.
- (8) Stockmayer, W. H.; Fixman, M. *Ann. N. Y. Acad. Sci.* **1952**, *57*, 334.
- (9) de Gennes, P.-G. *Physica (Utrecht)* **1959**, *25*, 825.
- (10) Khasat, N.; Pennisi, R. W.; Hadjichristidis, N.; Fetters, L. J. *Macromolecules* **1988**, *21*, 1100.
- (11) Benoit, H. *J. Polymer Sci.* **1953**, *11*, 507.
- (12) Huber, K.; Bantle, S.; Burchard, W.; Fetters, L. J. *Macromolecules* **1986**, *19*, 1404.
- (13) Huber, K.; Burchard, W.; Bantle, S.; Fetters, L. J. *Polymer* **1987**, *28*, 1900, 1997.
- (14) Mezei, F. In *Lecture Notes in Physics*; Mezei, F., Ed.; Springer-Verlag: Berlin, Heidelberg, New York, 1980; Vol. 128.
- (15) Dubois-Violette, E.; de Gennes, P.-G. *Physica (Long Island City, N. Y.)* **1967**, *3*, 181.
- (16) Witten, T. A.; Pincus, P. A.; Cates, M. E. *Europhys. Lett.* **1986**, *2*, 137.
- (17) Nicholson, L. K.; Higgins, J. S.; Hayter, J. B. *Macromolecules* **1981**, *14*, 836.
- (18) Mas, J. W.; Hadjichristidis, N.; Fetters, L. J. *Macromolecules* **1985**, *18*, 2330.
- (19) Hadjichristidis, N.; Xu, C.; Fetters, L. J.; Roovers, J. J. *Polym. Sci., Polym. Phys. Ed.* **1982**, *20*, 743.
- (20) Nicholson, L. K.; Higgins, J. S.; Hayter, J. B. *Proceedings of the 27th International Symposium on Macromolecules*; Strasbourg, July 6-9, 1981.

## Chain Configurations in Semicrystalline Interphases: Chain Stiffness

J. A. Marqusee

*Polymers Division, National Bureau of Standards, Gaithersburg, Maryland 20899, and Institute for Defense Analyses, 1801 N. Beauregard Street, Alexandria, Virginia 22311.*  
Received February 24, 1988; Revised Manuscript Received June 27, 1988

**ABSTRACT:** A previously presented mean-field lattice theory (*Macromolecules* **1986**, *19*, 2420) is extended to treat chain stiffness. The effect of bending energy on the configurational properties of chains at semicrystalline interfaces is analyzed. The width of the interfacial region and the degree of adjacent reentry are presented as a function of chain stiffness. A comparison with the case of chains bounded by a hard wall is given.

## Introduction

The configurations of long-chain molecules at the crystal/amorphous interface in semicrystalline polymeric materials has been actively debated for a number of years.<sup>1-3</sup> A melt of long-chain molecules when cooled forms a series of lamellar crystals which are separated by

amorphous regions. The chains can be many times longer than the width of these lamellae and thus they may possibly traverse the crystal and amorphous regions many times.

A large number of the chains which exit the crystal must reenter it so as to avoid an anomalously high density in